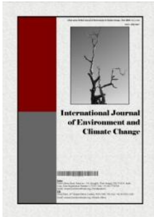

International Journal of Environment and Climate Change

10(10): 147-156, 2020; Article no.IJECC.61830
ISSN: 2581-8627
(Past name: British Journal of Environment & Climate Change, Past ISSN: 2231–4784)

Use of Sentinel-1 Data in Flood Mapping in the Buna River Area

Freskida Abazaj[1*] and Gëzim Hasko[1]

[1]Department of Geodesy, Faculty of Civil Engineering, Polytechnic University of Tirana, Albania.

Authors' contributions

This work was carried out in collaboration between both authors. FA designed the study, performed the statistical analysis, wrote the protocol and wrote the first draft of the manuscript. GH managed the analyses of the study and the literature searches. Both authors read and approved the final manuscript.

Article Information

DOI: 10.9734/IJECC/2020/v10i1030257
Editor(s):
(1) Dr. Sarfraz Hashim, Muhammad Nawaz Shareef University of Agriculture, Pakistan.
Reviewers:
(1) Hassan Kamil Jassim, University of Thi-Qar, Iraq.
(2) Mehmet Ozyazicioglu, Ataturk University, Turkey.
(3) Sanat Kumar Dwibedi, Odisha University of Agriculture and Technology (OUAT), India.
Complete Peer review History: http://www.sdiarticle4.com/review-history/61830

Original Research Article

Received 02 August 2020
Accepted 09 October 2020
Published 23 October 2020

ABSTRACT

Floods are one of the disasters that cause many human lives and property. In Albania, most floods are associated with periods of heavy rainfall. In recent years, Synthetic Aperture Radar (SAR) sensors, which provide reliable data in all weather conditions and day and night, have been favored because they eliminate the limitations of optical images.
In this study, a flood occurred in the Buna River region in March 2018, was mapped using SAR Sentinel-1 data. The aim of this study is to investigate the potential of flood mapping using SAR images using different methodologies. Sentinel-1A / B SAR images of the study area were obtained from the European Space Agency (ESA).
Preprocessing steps, which include trajectory correction, calibration, speckle filtering, and terrain correction, have been applied to the images. RGB composition and the calibrated threshold technique have been applied to SAR images to detect flooded areas and the results are discussed here.

Keywords: Flood; SAR image; RGB composite; pre-processing; thresholds technique.

**Corresponding author: E-mail: freskida.abazaj@fin.edu.al;*

1. INTRODUCTION

A river flood occurs when the flow no longer contains within its bed and over spills its banks. Flooding is a natural hazard, caused by heavy rainfall, peak seasonal rains, or seasonal snow melt [1].

The European Environment Agency (EEA) [2] found that from 1980 to 2010, European countries registered 3563 floods in total. Analyzes of data on these floods indicate significant increases in flooding and predict that flood losses will increase fivefold as a result of climate change, increased urban development and the price of land around the floodplains. [3,4] Remote sensing techniques are an effective source of information for discriminating water masses over large areas and can therefore be used to design flooded surfaces with sufficient temporal and spatial resolution [3,5].

In Albania, most floods are associated with periods of heavy rain. The validity of multispectral observations for this purpose is limited by clouds because unclear weather conditions often occur during floods. [6]. However, synthetic aperture radar (SAR) is a form of radar that is used to create more useful images over a target area to provide fine-grained spatial resolution, which can operate day and night and is unaffected by cloud cover, smoke, atmospheric water or hydrometeors [3,7,8,9]. Sentinel-1 satellite, operated by ESA's Copernicus program, consists of two satellite sensors (Sentinel-1A / B) with a repeat cycle of 6 days. Each Sentinel-1 satellite has a C-Band SAR sensor operating at 5.405 GHz. They have 4 operating modes with different extents, polarizations, incidence angles and resolutions: Strip map (SM), Interferometric Wide Area (IW), Extra Wide (EW) and Wave. By default, they provide data in IW mode that dual polarized SAR data with VV and VH polarization [3,10,11]. This method was applied in the case of floods that occurred in the month of March 2018 in Buna River due to the melting snow and the heavy rainfall. The main objective of this study is to map the extent of a flood using Sentinel-1 data. For this, two different Sentinel-1 datasets were obtained from ESA's Copernicus Open Access Hub and pre-processed using the SNAP tool provided free of charge for radiometric and geometric calibration and noise filtering.

For mapping the non-permanent water surfaces, there are two detection algorithm approaches (RGB composition and Calibration Threshold technique) of free water surfaces to derive flood mapping from SAR images.

2. MATERIALS AND METHODOLOGY

The project area is located in Northwestern Albania on the border with Montenegro. It is characterized by the coastal plain of the rivers Drin and Buna, the surrounding mountains - at the foot of the Albanian Alps - up to more than 1,700 m (Cukali Mountain, east of Shkodra) and Lake Shkodra, a large inland lake which is divided between the two countries Albania and Montenegro. The Buna River at the southern end of the lake is the only outlet that flows into the Adriatic Sea after joining the Drin River near the city of Shkodra. Floods are frequent during the period November-March, when the region receives about 80-85 percent of annual rainfall [12]. This potential risk area in the Shkodra region covers the municipalities of Ana e Malit, Bërdicë, Bushat, Dajç, Gur i Zi and Velipoja. The Buna River stretches from the outlet of Lake Shkodra to the Adriatic Sea and has a length of 44 km. In the last kilometers, before joining the sea, the Buna River flows partly along the border between Montenegro and Albania.

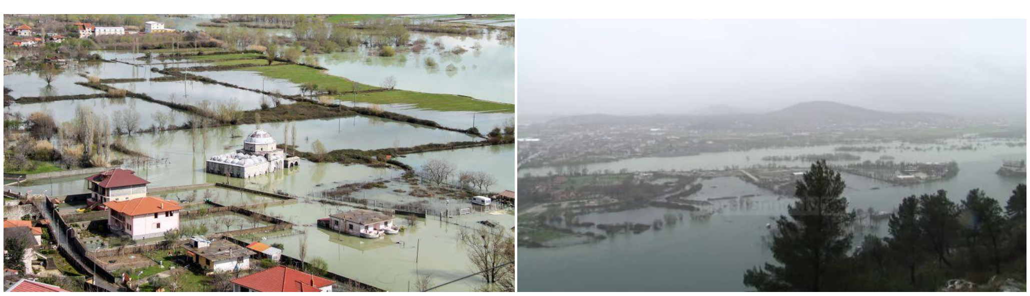

Fig. 1. Damage after the march flood in Shkodra caused by heavy rainfall in the country
(photo credits: https://www.euractiv.com/section/climate-environment/news/extreme-weather-events-on-the-rise-european-scientists-warn/- accessed on March 22th, 2018). (photo credits: http://top channel.tv/video/permbytet-durresi-uji-pushton-rruget/ - accessed on March 19th, 2018)

2.1 Sentinel -1 Datasets

Sentinel-1 SAR data was used in this study. Sentinel-1 satellite constellation consists of Sentinel-1A and Sentinel-1B, which share the same orbital plane. They carry a synthetic aperture C-band radar instrument that provides a collection of data in all weather conditions, day and night. This instrument has a spatial resolution of up to 5 m and a band of up to 400 km. Sentinel-1A and Sentinel-1B were launched by ESA on April 3, 2014 and April 25, 2016 respectively [3,13]. The re-visit time of each satellite (Sentinel-1A and Sentinel-1B) is 12 days, which means 6 days for the combined constellation [3,14] and can be considered a long visit time. The data obtained from the Sentinel-1 sensors has 4 different modes with different resolutions, extents, polarizations and angles of incidence: Strip Map (SM), Interferometric Wide Area (IW), Extra Wide (EW) and Wave. In this study, two Sentinel-1 SAR images collected in IW area mode were used. This mode is the main land acquisition mode and has single and double polarizations (VV: vertical send - vertical receive; and VH: vertical send - horizontal receive) [3,15]. Data obtained under one wet (DS-1) and one dry (DS-2) weather conditions were selected for the studies. The Sentinel-1 images used here are made available free of charge from the Scientific ESA Data Center website [3,16]. The Sentinel-1 images are provided in Ground Range Detected (GRD) format with an original 20 m x 22 m spatial resolution for range and azimuth, and they are all acquired in descending trajectory direction. The GRD data has been resampled to a ground pixel size of 10 mx 10 m [3,17]. The main features of the SAR datasets used in the study are presented in Table 1. As summarized in the table, the first dataset (DS-1) was obtained on March 18, 2018 during the flood. The second data set (DS-2) was acquired on August 8, 2017 to create reference data for non-flooding situations.

2.2 Methodology

An overall workflow of the methodology used here is provided in Fig. 3.

Table 1. Characteristics of the SAR datasets used in the study

ID	Acquisition Date	Data Format and Mode	Acquisition Model	Weather
DS-1	18 March 2018	GRD-IW	VV+VH	wet
DS-1	8 August 2017	GRD-IW	VV+VH	dry

Fig. 2. Extents of the SAR data used in the study (DS-1, DS-2) and the sub-area (3) used for flood mapping

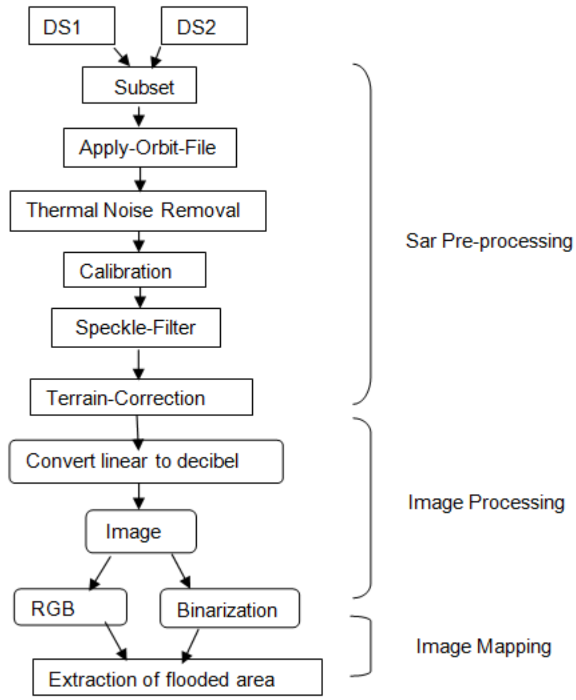

Fig. 3. Flowchart of the methodology

2.2.1 SAR sentinel-1 data pre-processing

SAR polarization is an essential factor in flood detection [3,18]. VV-polarized images are considered more suitable for the detection of floods and water bodies than VH in several previous studies [3,19-22]. For this reason, VV polarized images have been used in this study. The images were processed with the free software SNAP (Sentinel Application Platform) Tool [3,23], created by ESA for the analysis of the data captured by Sentinel satellites.

Thermal noise affects the quality of the images, especially in areas with low backscatter, such as calm seas and lakes. Therefore, thermal noise was removed in this step using the SNAP Toolbox. Precise orbit file was used because the orbit file provides accurate information about the satellite position and speed. (SNAP Help). Calibration is required for quantitative analysis of SAR images acquired from different sensors or at different times from the same sensor. Therefore radiometric calibration has been applied and σ0 (sigma zero) values are obtained in decibels (dB). The pixels representing water bodies have a smaller backscatter coefficient σ0 compared to other features. One of the problems facing SAR images is speckle noise caused by the random effects of the multiple backscatters that occur in each resolution cell. Speckle noise is a type of noise that reduces the quality of an image and can make visual or digital interpretation more difficult, so it is generally desirable to reduce it before interpretation and analysis [3,24,25].

The speckle filter application does not change the spatial details and is usually used to smooth the boundaries of the different shapes displayed, avoiding the loss of image details. The Gamma Map filter is based on Bayes' statistical analysis of the image and works best for extensive areas, such as oceans, forests or vast fields [26]. The Lee filter uses statistical parameters, such as the mean and standard deviation, with a predetermined window size that assesses various smoothing factors. In homogeneous areas, such as flooded areas, the final pixel value is the linear average of adjacent pixels [27]. The Refined Lee filter creates a softer texture in the image, minimizing radiometric and texture loss in the images [28,29]. The Lee Sigma filter uses a statistical distribution of the digital levels of a particular area window selected by the operator and estimates which pixel to consider [30]. Taking into account the polarization and the need to delimit those areas with smaller intensity values, the Lee filter with a window size of 7m x 7m was chosen as the most suitable for the study. The last step in image preprocessing is to perform terrain correction. This primarily eliminates distortions due to changes in topography and incidence angle with the ground from the nadir. The geometric calibration used in this study was Range Doppler terrain Correction and the Digital Elevation Model (DEM) –SRTM-3Sec [3].

2.2.2 SAR sentinel-1 data processing

In this study, the methodologies used were the RGB composition and the calibrated threshold technique. RGB composition is a suitable method for visualizing multi-temporal changes and facilitates detection of changes on the ground surface through a temporal color image [31]. It is a method based on the differences between pre- and post-event images, and in which a combination of bands is established so that these differences become visually noticeable. These differences are determined by the change in the intensity value for the same pixel on different dates. The result is a multi-temporal image with a band assigned to each of the primary colors to form an RGB composite image.

The other method used was the threshold calibration technique. It is a quick and easy process that distinguishes which areas are flooded from areas that are not flooded by generating histograms .The use of this method is not recommended for rapid flash floods, where mapping of the map is urgent and the presence of noise causes some uncertainty [3,32,33]. Knowing that backscatter values in permanent waters and in flooded areas are usually the most negative and differ markedly from subsequent radiometric values caused by other physical changes, it is possible to set limit [34].

In this way, the threshold could be manually adjusted between areas that were flooded and those that were not. Later, using a mathematical equation of the bands, a new two-color image separating the two areas was produced. Later, using a mathematical equation of the bands, a new two-color image was created separating the two areas [35].

3. RESULTS AND DISCUSSION

3.1 RGB Composition Results

We applied a technique to distinguish between flooded areas and the permanent water body and to do this we will create an RGB composite. In the red band we select the image before the flood and in the blue and green band we select the crisis image.

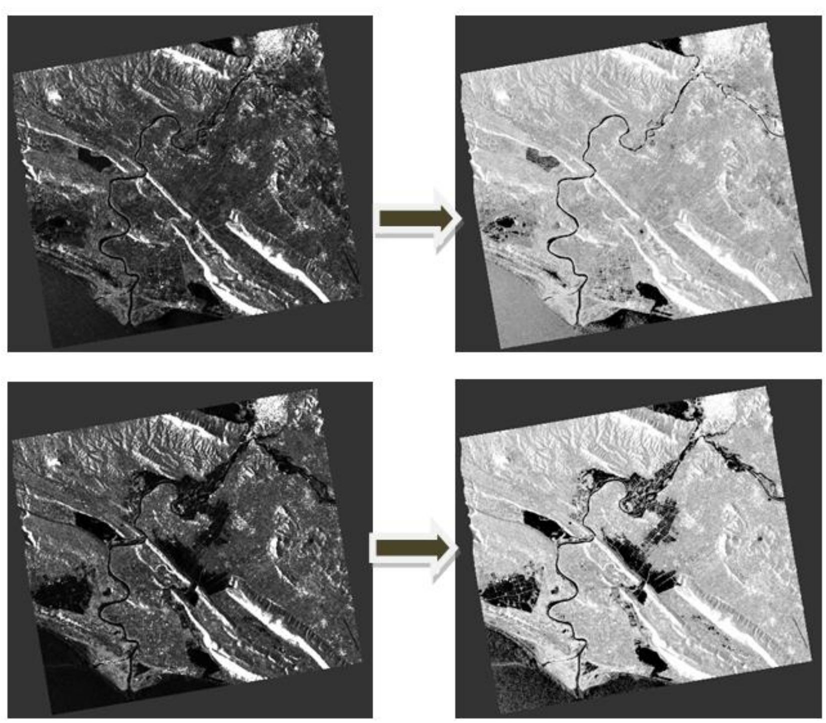

Fig. 4. The linear pre-processed images (before and after flood) convert in dB

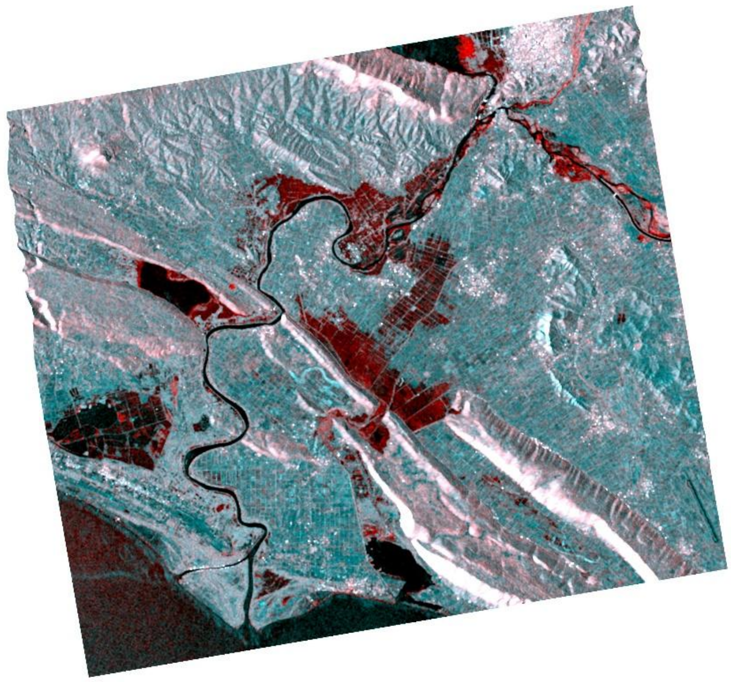

Fig. 5. The RGB composition of study area

In the read channel, we will have a high radar response to the flooded areas because these areas will be land. In the dry image, we do not expect flooded areas and therefore will have high backscatter efficiency. However, on the flooded areas, there will be a weak backscattering return in the image of the crisis, so when we see the flooded areas, they should appear red because they will have a high response in the red channel but a low response in green and blue channels. Above the surrounding areas where we don't have flooded areas we should see shades of gray, as the backscatter should be more or less the same in red and blue. On permanent water bodies, we should have a uniform dark return, as there will be little backscatter to the wet and dry image. Therefore, in red, green and blue there will be a weak response. In the red areas, the river looks very dark and the surrounding areas have different shades of gray. In some areas we can see some parts of the image in cyan, so in the green and blue channels where we have a higher response in the wet image than in the dry image, but it could be due to some coverage of special soil that has nothing to do with flooding.

3.2 Threshold Technique Results

Two methods were used to preprocess the SAR images and thus improve them for further processing: (1) binarization by selecting two thresholds for the detection of wetlands, and (2) taking image differences (between images before and during the events). Threshold values are determined from analysis of pre-event data sets (mean of DS-2). The arithmetic difference between the threshold image of DS-1 and the average image produced in the previous step was calculated to determine the areas of change. The threshold method (histogram threshold) is a simple, but widely used and efficient method to generate binary images [34]. Here, the threshold method is used to delineate water from non-water. For this, the histogram of the filtered backscatter coefficient showing the Buna River and its surroundings was analyzed. The low values of the backscatter histogram correspond to water and the high values correspond to the waterless class (Fig. 6).

As a result of the visual investigations of arithmetic mean of pre-event images, the pixel values of the water areas have been determined to be between -217 and -13 dB. After studying the results, we conclude that the threshold taken was -16.5 dB in the image before flood and -14.11 dB in the image during flood. At the end we have visualize and create a map of flooded area in Buna River with QGIS software. As base map we have selected the world map.

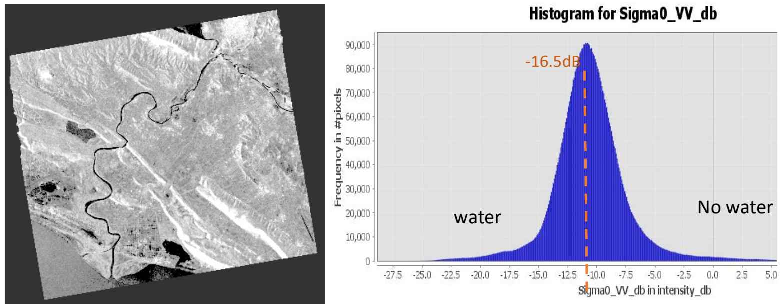

Fig. 6. Preprocessed image and histogram of date 08/08.2017 before flooding

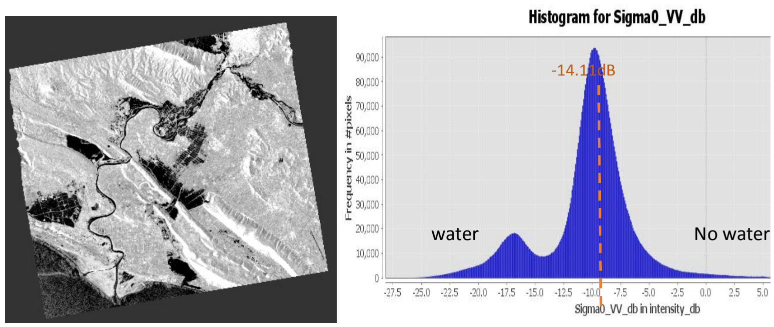

Fig. 7. Preprocessed image and histogram of date 18/03.2018 during flooding

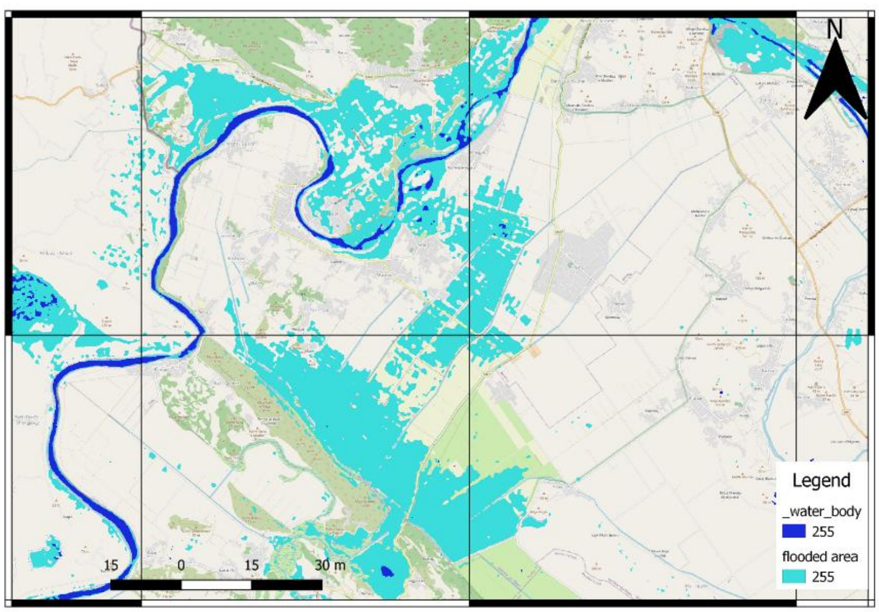

Fig. 8. Flood map in Buna River Area

4. CONCLUSION

In this study, a methodology derived from SAR images was proposed for flood monitoring. The data used were the Sentinel-1 SAR databases of the European Earth Observation mission to monitor the floods occurring in the Buna River (Albania) in March 2018. In SAR images, inland waters exhibit a strong contrast in backscatter values due to their low roughness or zero in the absence of waves, behaving like a special surface that reflects the radar return signal in a direction opposite to the position of the sensor. However, they need a correction and filtering process. By evaluating the different Sentinel-1 parameters, our analysis showed that the best results were obtained using the VV polarization configuration. Two methods were applied to detect and determine non-permanent water surfaces from Sentinel-1 SAR images. The first method of RGB composition is based on the differences between the images before and after the event, in which a combination of bands is placed to identify these changes as visually prominent. The threshold technique is based on a quick and simple process that differentiates flooded areas from those not taken from the characteristic polarization histogram using backscatter values in standing water and flooded areas. The advantage of using the RGB composition methodology is that a clear distinction is made between permanent and temporarily flooded areas, while achieving the difference through the calibration threshold technique requires other processes.

COMPETING INTERESTS

Authors have declared that no competing interests exist.

REFERENCES

1. Po NL. Ecological response to and management of increased flooding caused by climate change. Philos. Trans. A Math. Phys. Eng. Sci. 2002;360:1497–1510.
2. European Environment Agency. Flood risks and environmental vulnerability; Exploring the synergies between floodplain restoration, water policies and thematic policies. European Environment Agency: Copenhagen, Denmark. 2016;9–15.
3. Carreño Conde F. De Mata Muñoz M. Flood monitoring based on the study of sentinel-1 SAR Images: The Ebro River Case Study. Water. AMA Style. 2019; 112454. Available:https://www.mdpi.com/20734441/11/12/2454/htm
4. Merz B, Aerts J, Arnbjerg-Nielsen K, Baldi M, Becker A, Bichet A, Blöschl G, Bouwer LM, Brauer,A, Cio F, et al. Floods and climate: Emerging perspectives for flood risk assessment and management.Nat. Hazards Earth Syst. Sci. 2014;14:1921–1942.
5. Bioresita F, Puissant A, Stumpf A, Malet JF. Fusion of sentinel-1 and sentinel-2 image time series for permanent and temporary surface water mapping. Int. J. Remote Sens. 2019;40:9026–9049.
6. Shen X, Wang D, Mao K, Anagnostou E, Hong Y. Inundation extent mapping by synthetic aperture radar: A review. Remote. Sens. 2019;11:879.
7. Tomer ST, Al Bitar A, Sekhar M, Zribi M, Bandyopadhyay S, Sreelash K, Sharma AK, Corgne S, Kerr Y. Retrieval and multi-scale validation of soil moisture from multi-temporal SAR data in a semi-arid tropical region. Remote Sens. 2015;7:8128–8153.
8. Filion R, Bernier M, Paniconi C, Chokmani K, Melis M, Soddu A, Talazac M, Lafortune FX. Remote sensing for mapping soil moisture and drainage potential in semi-arid regions: Applications to the Campidano plain of Sardinia, Italy. Sci. Total Environ. 2016;573:862–876.
9. Zhang B, Wdowinski S, Oliver-Cabrera T, Koirala R, Jo MJ, Osmanoglu B. Mapping the extent and magnitude of sever flooding induced by hurricane IRMA with multi-temporal SENTINEL-1 SAR and insar observations. ISPRS-International Archives of the Photogrammetry, Remote Sensing and Spatial Information Sciences. 2018;2237-2244, Available:https://doi.org/10.5194/isprsarchives-XLII-3-2237-2018
10. Cazals C, Rapinel S, Frison PL, Bonis A, Mercier G, Mallet C, Corgne S, Rudant JP. Mapping and characterization of hydrological dynamics in a coastal marsh using high temporal resolution Sentinel-1A images. Remote Sensing. 2016;8(7):570. DOI: 10.3390/rs8070570
11. Torres R, Snoeij P, Geudtner D, Bibby D, Davidson M, Attema E, Potin P, Rommen B, Floury N, Brown M. GMES Sentinel-1 mission. Remote Sensing of Environment, 2012;120:9–24. Available:https://doi.org/10.1016/j.rse.2011.05.028
12. Bogdani M. Risk assessment from floodings in the rivers of Albania. Int. Conf. on Destructive Water, Anaheim, 1996;24-28:83-85.
13. Comprehensive review and outlook to Sentinel-1. Remote Sensing. 2014;6:4870–4906. Available:https://doi.org/10.3390/rs6064870

14. Nagler T, Rott H, Ripper E, Bippus G, Hetzenecker M. Advancements for snowmî. Sentinel-1-based flood mapping: A fully automated processing chain. International Journal of Remote Sensing. 2016;37(13):2990–3004. Available:https://doi.org/10.1080/01431161.2016.1192304
15. Cazals C, Rapinel S, Frison PL, Bonis A, Mercier G, Mallet C, Corgne S, Rudant JP. 2016. Mapping and characterization of hydrological dynamics in a coastal marsh using high temporal resolution Sentinel-1A images. Remote Sensing 2016;8(7):570. DOI: 10.3390/rs8070570
16. EO Browser; 2020. Available:https://apps.sentinel-hub.com/eo-browser
17. Torres R, Snoeij P, Geudtner D, Bibby D, Davidson M, Attema E, Potin P, et al. GMES Sentinel-1 Mission. Remote Sensing of Environment. 2012;120:9–24. DOI: 10.1016/j.rse.2011.05.028.
18. Psomiadis E. Flash flood area mapping utilizing Sentinel-1 radar data. In proceedings of the earth resources and environmental remote sensing/GIS Applications VII, Edinburgh, UK. 2016;26–29 DOI: 10.1117/12.2241055
19. Twele A, Cao WX, Plank S, Martinis S. Sentinel-1-based flood mapping: a fully automated processing chain. International Journal of Remote Sensing. 2016;37(13): 2990–3004. Available:https://doi.org/10.1080/01431161.2016.1192304
20. Henry JB, Chastanet B, Fellah K, Desnos YL. Envisat multi-polarized ASAR data for flood mapping. International Journal of Remote Sensing. 2006;27(10):1921-1929. Available:https://doi.org/10.1080/01431160500486724
21. Clement MA, Kilsb G, Moore P. Multi-temporal synthetic aperture radar flood mapping using change detection. Journal of Flood Risk Management. 2017;39:130-152-168. Available:https://doi.org/10.1111/jfr3.12303
22. Manjusree R, Kumar LP, Bhatt CM, Rao GS, Bhanumurthy V. Optimization of threshold ranges for rapid flood inundation mapping by evaluating backscatter profiles of high incidence angle SAR images. International Journal of Disaster Risk Science. 2012;3(2):113–122. Available:https://doi.org/10.1007/s13753-012-0011-5
23. SNAP. Sentinel Application Platform; 2018. Available:http://step.esa.int/main/toolboxes/snap/
24. Singh P, Shree R. Analysis and effects of speckle noise in SAR images. In Advances in Computing, Communication, & Automation (Fall), ICACCA. 2016;2–6. DOI: 10.1109/ICACCAF.2016.7748978
25. Miranda N, Meadows PJ. Radiometric calibration of S-1 Level-1 products generated by the S-1 IPF, ESA-EOPG-CSCOP-TN-0002; European Space Agency: Paris, France; 2015.
26. Senthilnath J, Handiru V, Rajendra R, Omkar SN, Mani V, Diwakar P. Integration of speckle de-noising and image segmentation using synthetic aperture radar image for flood extent extraction. J. Earth Syst. Sci. 2013;122:559–572.
27. Park JM, Song WJ, Pearlman WA. Speckle filtering of SAR images based on adaptive windowing. IEE Proc. Vis. Image Signal Process. 1999;146:191–197.
28. Borah SB, Sivasankar T, Ramya MNS, Raju PLN. Flood inundation mapping and monitoring in Kaziranga National Park, Assam using Sentinel-1 SAR data. Environ. Monit. Assess. 2018;190-520.
29. Ezzine A, Darragi F, Rajhi H, Ghatassi A. Evaluation of sentinel-1 data for flood mapping in the upstream of Sidi Salem dam (Northern Tunisia). Arab. J. Geosci. 2018;11:170.
30. García R, González C, De la Vega R, Valverde A, Seben E. Análisis del Comportamiento de Filtros de Reducción de Speckle en Imágenes ERS2-SAR; Teledetección y Desarrollo Regional; X Congreso de Teledetección: Cáceres, Spain. 2003;325–328.
31. Amitrano D, Guida R, Ruello G. Multitemporal SAR RGB Processing for Sentinel-1 GRD Products: Methodology and Applications. IEEE J. Select. Top. Appl. Earth Obs. Remote Sens. 2019;12: 1497–1507.
32. Tavus B, Kocaman S, Gokceoglu C, Nefeslioglu HA. Considerations on the use of sentinel-1 data in flood mapping in urban areas: Ankara (Turkey) 2018 floods. Int. Arch. Photogramm. Remote Sens. Spat. Inf. Sci. 2018;43(5):575–581.
33. Westerho RS, Kleuskens MPH, Winsemius HC, Huizinga HJ, Brakenridge GR, Bishop C. Automated global water mapping based

on wide-swath orbital synthetic-aperture radar. Hydrol. Earth Syst. Sci. 2013;17:651–663.

34. Bioresita F, Puissant A, Stumpf A, Malet JP. A method for automatic and rapid mapping of water surfaces from Sentinel-1 imagery. Remote Sens. 2018; 10:217.

35. Pulvirenti L, Chini M, Pierdicca N, Guerriero L, Ferrazzoli P. Flood monitoring using multitemporal COSMO-SkyMed data: image segmentation and signature interpretation. Remote Sensing Environment. 2011;115(4):990–100. Available:https://doi.org/10.1016/j.rse.2010.12.002

Peer-review history:
The peer review history for this paper can be accessed here:
http://www.sdiarticle4.com/review-history/61830